EXPERIMENTAL GENERATION OF LONGITUDINALLY-MODULATED ELECTRON BEAMS USING AN EMITTANCE EXCHANGE TECHNIQUE *

Y.-E Sun[1], P. Piot[1,2], A. Johnson[3], A. Lumpkin[3], T. Maxwell[1,2], J. Ruan[3], and R. Thurman-Keup[3]
[1] Accelerator Physics Center, Fermi National Accelerator Laboratory, Batavia, IL 60510, USA
[2] Department of Physics, Northern Illinois University DeKalb, IL 60115, USA
[3] Accelerator Division, Fermi National Accelerator Laboratory, Batavia, IL 60510, USA

Abstract

We report our experimental demonstration of longitudinal phase space modulation using a transverse-to-longitudinal emittance exchange technique. The experiment is carried out at the A0 photoinjector at Fermi National Accelerator Lab. A vertical multi-slit plate is inserted into the beamline prior to the emittance exchange, thus introducing beam horizontal profile modulation. After the emittance exchange, the longitudinal phase space coordinates (energy and time structures) of the beam are modulated accordingly. This is a clear demonstration of the transverse-to-longitudinal phase space exchange. In this paper, we present our experimental results on the measurement of energy profile as well as numerical simulations of the experiment.

INTRODUCTION

Recent years have witnessed an increasing demand for precise phase-space control schemes. In particular, electron bunches with a well-defined temporal distribution are often desired. An interesting class of temporal distribution consists of a train of microbunches with sub-picosecond duration and separation. Applications of such trains of microbunches include the generation of super-radiant radiation [1] or the resonant excitation of wakefield in plasma wakefields accelerators or dielectric-loaded structures [2]. We have recently explored an alternative technique based on the use of a transverse-to-longitudinal phase space exchange method [3, 4]. The method consists of shaping the beam's transverse density to produce the desired horizontal profile. The horizontal profile is then mapped onto the longitudinal profile by a beamline capable of exchanging the phase space coordinates between the horizontal and longitudinal degrees of freedom. Therefore the production of a train of microbunches simply relies on generating a set of horizontally-separated beamlets upstream of the beamline. The backbone of the proposed technique is the transverse-to-longitudinal phase space exchange which was recently proposed as a means to mitigate the microbunching instability in high-brightness electron beams [5] or to improve the performance of single-pass FELs [6]. A simple optical lattice capable of performing this phase space exchange consists of a horizontally-deflecting cavity, operating on the TM_{110} mode, flanked by two horizontally-dispersive sections henceforth referred to as "doglegs" [7]. Under the thin lens approximation the initial transverse phase space coordinates (x_0, x_0') are mapped to the longitudinal phase space coordinates (z, δ) following [8]

$$\begin{cases} z = & -\frac{\xi}{\eta}x_0 - \frac{L\xi-\eta^2}{\eta}x_0' \\ \delta = & -\frac{1}{\eta}x_0 - \frac{L}{\eta}x_0', \end{cases} \quad (1)$$

where L is the distance between the dogleg's dipoles, and η and ξ are respectively the horizontal and longitudinal dispersions generated by one dogleg. The coupling described by Eq. 1 can be used to arbitrarily shape the temporal distribution of an electron beam [9].

EXPERIMENTAL SETUP

The experiment was carried out at the Fermilab's A0 Photoinjector [10] and the corresponding setup is discussed in Ref. [11]. A $\sim$ 16 MeV beam produced by a photoinjector can be directed to a "straight ahead" or emittance exchange (EEX) beamlines.

The "straight ahead" beamline incorporates an horizontally-bending spectrometer equipped with a cerium doped yttrium aluminum garnet (YAG:Ce) screen (henceforth referred to as XS3) for energy measurement. The horizontal dispersion value at XS3 location is $|\eta_{x,XS3}| = 317$ mm.

The other beamline, the emittance exchange (EEX) beamline, implements the aforedescribed double-dogleg emittance exchanger [12]. The doglegs consist of dipole magnets with $\pm 22.5^\circ$ bending angles and each generate a horizontal and longitudinal dispersions of $\eta \simeq -33$ cm and $\xi \simeq -12$ cm, respectively [1]. The deflecting cavity is a liquid-Nitrogen–cooled, normal-conducting, five-cell cavity operating on the TM_{110} π-mode at 3.9 GHz [13]. The lattice downstream of the EEX beamline includes three quadrupoles, a suite of standard beam diagnostics and a vertical spectrometer. Downstream of the EEX beamline, at X24, coherent transition radiation (CTR) generated as the beam impinges an Aluminum screen can be measured

* This work was supported by the Fermi Research Alliance, LLC under Contract No. DE-AC02-07CH11359 with the U.S. Department of Energy. P.P. was partially supported by the US Department of Energy under Contract No. DE-FG02-08ER41532 with Northern Illinois University.

[1] In our convention the head of the bunch is for $z < 0$.

using a bolometer. The vertical dispersion generated by the vertical spectrometer at the downstream XS4 YAG screen is $|\eta_{y,XS4}| = 944$ mm.

For the proof-of-principle experiment, the production of a transverse modulation was achieved by passing the beam through a set of remotely insertable vertical slits at X3. This multislit mask, nominally designed for single-shot transverse emittance measurements, consists of 50 μm wide slits made out of a 3-mm-thick tungsten plate. The slits are separated by 1 mm. Less than 5 % of the incoming beam is transmitted through the mask. This mask is obviously not optimized for the present experiment: a smaller slits spacing would be more beneficial to increase the total transmitted charge and to get a smaller separation between the bunches after the EEX beamline.

ENERGY MODULATIONS

The beam was first diagnosed in the straight-ahead line and the spectrometer to ensure especially that no energy modulation was observable. The resulting set of observations is depicted in Fig. 1.

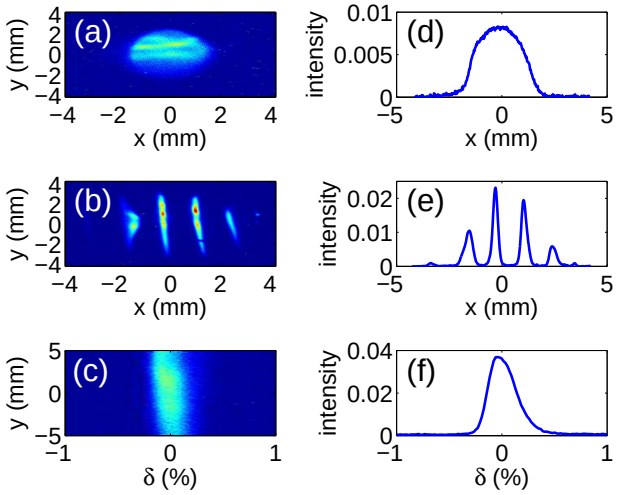

Figure 1: Characterization of the transversely modulated beam upstream of the emittance exchanger showing the beam transverse density at X3 (before inserting the multislit mask) (a), the beam density at X5 after insertion of the multislit mask at X3 (b), an example of beam energy spectrum measured at XS3 with X3 slits inserted (c). The plots (d, e, f) in the right column are the corresponding horizontal projections.

The beam was then transported through the EEX beamline. Powering the cavity to its nominal deflecting voltage resulted in the appearance of an energy modulation at XS4; see Fig. 2. These observations clearly demonstrate the ability of the EEX beamline to convert an incoming transverse density modulation into an energy modulation. In the present measurement the incoming horizontal Courant-Snyder (C-S) parameters at the EEX beamline entrance were empirically tuned to maximize the energy modulation. However other C-S parameters settings can map the initial modulation into a temporal modulation as can be inferred from Eq. 1.

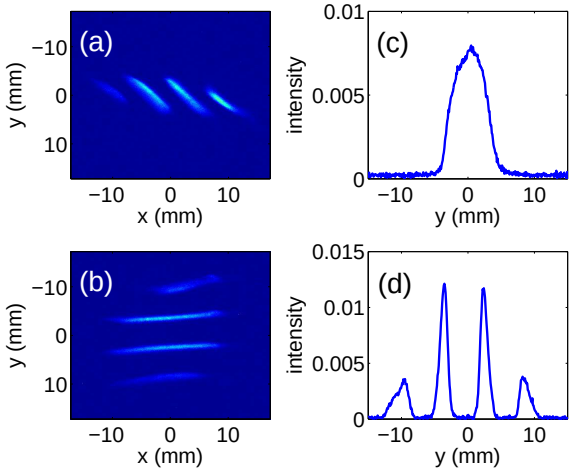

Figure 2: Characterization of the transversely modulated beam upstream of the emittance exchanger showing the beam transverse density at XS4 with the deflecting cavity off (a) and on (b), The plots (c,d) in the right column are the corresponding vertical projections. The vertical axis y is proportional to the fractional momentum spread.

Start-to-end simulations were performed in order to provide insight on the experimental results. The program ASTRA [14] was used to model the beam dynamics from the cathode to X3 using the same photoinjector settings as used during our experiment. The effect of the multislit mask was simulated and the resulting distribution was tracked up to XS4 using ELEGANT [15] without including collective effects. The quadrupoles upstream of the EEX beamline were empirically tuned following the experimental procedure resulting to simulations in qualitative agreement with the measurements [11]. The corresponding simulated longitudinal phase space downstream of the EEX beamline is shown in Fig. 3(a). The phase space is significantly correlated and therefore has both energy and temporal modulations.

TEMPORAL MODULATIONS

To characterize the expected temporal modulations we detect coherent transition radiation (CTR) shining out of a single-crystal quartz windows as the beam impinges an aluminum mirror. The spectral intensity radiated by a bunch of N electrons by the CTR process is related to the single electron intensity $\frac{dI}{d\omega}\big|_1$ via $\frac{dI}{d\omega}\big|_N = \frac{dI}{d\omega}\big|_1 [N + N^2|S(\omega)|^2]$ where $S(\omega)$ is the intensity-normalized Fourier transform of the normalized charge distribution $S(t)$ [16]. The CTR occurs at frequencies smaller than the cut off frequency $f_c \equiv c/\{2\pi\sigma_z[1 + [\sigma_\perp/(\gamma\sigma_z)]^2]^{1/2}\}$ where σ_z and $\sigma_\perp$ are respectively the bunch length and transverse size at the CTR radiator location (the beam is assumed to be cylindri-

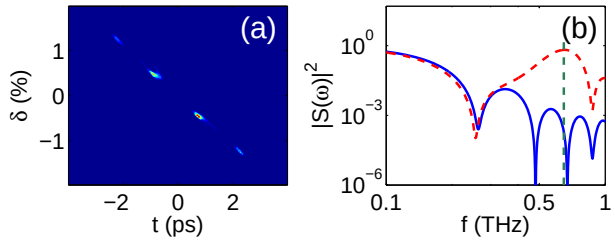

Figure 3: Simulated longitudinal phase space (t, δ) downstream of the EEX beamline (a) and resulting bunch form factor [red trace in plot (b)]. The blue trace in plot (b) is the bunch form factor computed for the entire beam (360 pC) at X24 i.e. when the X3 slits are not inserted. In image (a) $t > 0$ corresponds to the tail of the bunch.

cally symmetric). In addition if the bunch consists of a train of identical microbunches with periodicity τ the spectrum will be enhanced at frequencies $f_n = n/\tau$ (n is an integer). The CTR spectrum is representative of the temporal bunch distribution provided $\sigma_\perp \ll \gamma\sigma_z$. In addition imperfections due to the frequency-dependent transmissions of the THz beamline components alter the spectrum of the detected CTR. The computed bunch form factors (BFFs) $|S(\omega)|^2$ from the simulated macroparticle ensemble are shown in Fig. 3 for the case of the entire bunch, i.e. without slits X3 inserted, (blue solid trace) and for the case corresponding to image (a) of Fig. 3 (red dash trace). At $f_1 \simeq 0.7$ THz [indicated by the vertical green dash line in Fig. 3 plot (b)] the microbunch train BFF is strongly enhanced due to the intra-bunch coherence and is higher than the single bunch BFF.

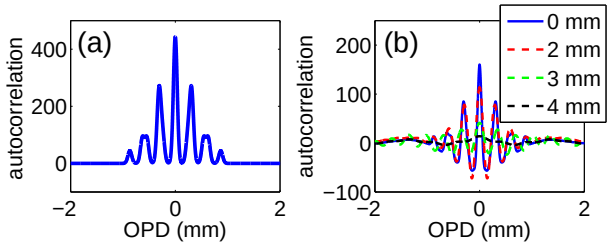

Figure 4: Simulated autocorrelation functions versus optical path difference (OPD) without (a) and including (b) frequency dependent transmission of the THz beamline elements. In plot (b) the traces corresponds to four values of $\sigma_\perp$ (for these simulations $\gamma = 30$).

In our experiment the CTR is collimated by an off-axis parabolic mirror and sent to a Michelson autocorrelator. The autocorrelated signal is detected using a He-cooled bolometer. A train of N microbunches is expected to yield an autocorrelation function with $2N - 1$ peaks; see Fig. 4 (a). To date we successfully measured the autocorrelation function associated to the beams discussed in the previous section with estimated charge ≤ 20 pC. However we have not been able to observe a multi-peaked autocorrelation function. We briefly elaborate on possible causes. Firstly only frequencies in the band $[0.1, 3]$ THz are transmitted through the system (the upper frequency limit comes from the crystal quartz vacuum windows) this should not affect our ability to resolve the multibunch structure but would prevent us from measuring the size of each microbunch; see blue trace in Fig. 4 (b). Another possible cause comes from the large transverse beam size at the CTR radiator location. As shown in Fig. 4 (b), the autocorrelation function amplitude weakens and its multi-peaked features eventually washes out as the transverse spot size increases. The transverse spot size on the CTR radiator could not be monitored during the experiment due to technical difficulties. However the large horizontal transverse emittance downstream of the exchanger ($\gamma\varepsilon_x \simeq 20$ μm with typical betatron functions $\beta \simeq 10 - 20$ m can easily results in transverse rms beam sizes in excess of 2 mm. In the next round of experiment, we plan on carefully monitoring and minimizing the transverse beam size. Based on our calculations this should insure the observation of multi-peaked autocorrelation functions. In addition, we plan to upgrade the crystal quartz vacuum window to a diamond window thereby allowing the transmission of higher frequencies. Such an improvement should enable the precise measurement of the microbunch lengths within the train.

We are indebted to W. Muranyi, J. Santucci, and B. Tennis for their excellent operational and technical supports. We thank M. Church, H. Edwards, E. Harms and V. Shiltsev for their interest and encouragement.

REFERENCES

[1] A. Gover, *Phys. Rev. ST Accel. Beams* **8**, 030701 (2005).

[2] C. Jing, *et al.*, *Phys. Rev. Lett.* **98**, 144801 (2007).

[3] P. Piot, *et al.*, AIP Conf. Proc. **1086**, 677 (2009).

[4] Y.-E Sun, and P. Piot, Proc. LINAC08, 498 (2009).

[5] M. Cornachia, and P. Emma, *Phys. Rev. ST Accel. Beams* **6** 030702 (2003).

[6] P. Emma, Z. Huang, K.-J. Kim, and P. Piot, *Phys. Rev. ST Accel. Beams* **9**, 100702 (2006).

[7] K.-J. Kim and A. Sessler, AIP Conf. Proc. **821**, 115 (2006).

[8] Y.-E Sun, *et al*, Proc. PAC07, 3441 (2007).

[9] P. Piot, *et al.*, to be published; preprint FERMILAB-PUB-09-265-APC (2010).

[10] J.-P. Carneiro, *et al.*, *Phys. Rev. ST Accel. Beams* **8**, 040101 (2005).

[11] Y.-E Sun *et al.*, arXiv:1003.3126v1 (2010).

[12] T. Koeth, *et al*, Proc. PAC09, FR5PFP020 (2009).

[13] T. W. Koeth, *et al*, ibid [8], 3663 (2007).

[14] `http://www.desy.de/~mpyflo/AstraDokumentation`.

[15] M. Borland, Advanced Photon Source LS-287, September 2000 (unpublished).

[16] J. S. Nodvick and D. S. Saxon, *Phys. Rev.* **96**, 180 (1954).